Automatic Face Reenactment

Pablo Garrido[1] Levi Valgaerts[1] Ole Rehmsen[1] Thorsten Thormählen[2]
Patrick Pérez[3] Christian Theobalt[1]
[1]MPI for Informatics [2]Philipps-Universität Marburg [3]Technicolor

Abstract

We propose an image-based, facial reenactment system that replaces the face of an actor in an existing target video with the face of a user from a source video, while preserving the original target performance. Our system is fully automatic and does not require a database of source expressions. Instead, it is able to produce convincing reenactment results from a short source video captured with an off-the-shelf camera, such as a webcam, where the user performs arbitrary facial gestures. Our reenactment pipeline is conceived as part image retrieval and part face transfer: The image retrieval is based on temporal clustering of target frames and a novel image matching metric that combines appearance and motion to select candidate frames from the source video, while the face transfer uses a 2D warping strategy that preserves the user's identity. Our system excels in simplicity as it does not rely on a 3D face model, it is robust under head motion and does not require the source and target performance to be similar. We show convincing reenactment results for videos that we recorded ourselves and for low-quality footage taken from the Internet.

1. Introduction

Face replacement for images [5, 4] and video [24, 2, 9] has been studied extensively. These techniques substitute a face or facial performance in an existing target image or video with a different face or performance from a source image or video, and compose a new result that looks realistic. As a particularly challenging case, *video face reenactment* replaces a face in a video sequence, while preserving the gestures and facial expressions of the target actor as much as possible. Since this process requires careful frame-by-frame analysis of the facial performance and the generation of smooth transitions between composites, most existing techniques demand quite some manual interaction.

In this paper, we present an entirely image-based method for video face reenactment that is fully automatic and achieves realistic results, even for low-quality video input, such as footage recorded with a webcam. Given an existing *target sequence of an actor* and a self-recorded *source sequence of a user* performing arbitrary face motion, our approach produces a new *reenacted* sequence showing the facial performance of the target actor, but with the face of the user inserted in it. We adhere to the definition of face replacement given by Dale *et al*. [9] and only replace the actor's inner face region, while conserving the hair, face outline, and skin color, as well as the background and illumination of the target video. We solve this problem in three steps: First, we track the user and the actor in the source and target sequence using a 2D deformable shape model. Then, we go over the target sequence and look in the source sequence for frames that are both similar in facial expression and coherent over time. Finally, we adapt the head pose and face shape of the selected source frames to match those of the target, and blend the results in a compositing phase.

Our reenactment system has several important advantages: 1) Our 2D tracking step is robust under moderate head pose changes and allows a freedom in camera view point. As opposed to existing methods, our system does not require that the user and the target actor share the same pose or face the camera frontally. 2) Our matching step is formulated as an image retrieval task, and, as a result, source and target performances do not have to be similar or of comparable timing. The source sequence is not an exhaustive video database, but a single recording that the user makes of himself going through a short series of non-predetermined facial expressions. Even in the absence of an exact match, our system synthesizes plausible results. 3) Our face transfer step is simple, yet effective, and does not require a 3D face model to map source pose and texture to the target. This saves us the laborious task of generating and tracking a personalized face model, something that is difficult to achieve for existing, prerecorded footage. 4) None of the above steps needs any manual interaction: Given a source and target video, the reenactment is created automatically.

We further make the following contributions: 1) We introduce a novel distance metric for matching faces between videos, which combines both appearance and motion information. This allows us to retrieve similar facial expressions,

while taking into account temporal continuity. 2) We propose an approach for segmenting the target video into temporal clusters of similar expression, which are compared against the source sequence. This stabilizes matching and assures a more accurate image selection. 3) A final contribution is an image-based warping strategy that preserves facial identity as much as possible. Based on the estimated shape, appearance is transferred by image blending.

The paper is organized as follows: Sec. 2 and 3 discuss related work and give a brief overview of our system. Sec. 4, 5, and 6 describe the three main steps in our pipeline. In Sec. 7, we present results and a validation for existing and self-recorded footage, before concluding in Sec. 8.

2. Related Work

Face replacement for image and video can be roughly divided into two categories. A first category is *facial puppetry* [24, 23, 26, 14, 21, 16], which aims to transfer expressions and emotions of a user (puppeteer) to a virtual character (puppet). Such methods are used to animate digital avatars in games, movies and video conferences. *Face swapping* methods [6, 5, 4, 13, 2, 9], on the other hand, try to exchange two faces in different images or videos such that the replaced result looks sufficiently realistic. Swapping different faces is useful for online identity protection, while swapping the same face (or parts of it) between different videos is interesting for dubbing, retargeting and video montage. At the intersection of both categories lies *face reenactment* [9], which replaces an actor's face by swapping it with that of a user, while at the same time preserving the actor's facial expressions and emotions. Here, the original facial performance needs to be accurately emulated (puppetry), and the new face with different identity needs to be inserted as naturally as possible in the original video (swapping).

Methods for face replacement in video can be further divided based on the underlying face representation:

A first type of methods tracks a morphable 3D model of the face that parameterizes identity, facial expressions and other nuances. Such systems can produce accurate 3D textured meshes and can establish a one-to-one expression mapping between source user and target actor, thereby simplifying and speeding up expression transfer. The generation of such a model, however, can be time consuming and is either done by learning a detailed 3D multilinear model from example data spanning a large variety of identities and expressions [24, 9], or by purposely building a person-specific blend shape model from scans of a specific actor using specialized hardware [11, 13, 2, 26, 25]. Moreover, the difficulty of stably tracking a 3D model over time generally necessitates a fair amount of manual interaction.

A second type of approaches finds similarities in head pose and facial expression between two videos solely based on image information. These image-based methods track the face using optical flow [16] or a sparse set of 2D facial features [21], and often include an image matching step to look up similar expressions in a database [14, 16]. Many image-based face replacement systems do not allow much head motion and assume that the actors in both videos share a similar frontal head pose [16]. As a result, substantial differences in pose and appearance may produce unrealistic composites or blending artifacts. If the task is to create a new facial animation, additional temporal coherence constraints must be embedded in the objective to minimize possible in-between jumps along the sequence [15, 3].

As far as we are aware, only the 3D morphable model technique of Dale *et al*. [9] could be used for face reenactment thus far. Their approach uses complex 3D mesh tracking, is not fully automatic, requires comparable source and target head poses, and was mainly demonstrated on sequences of similar performance. Our method, on the other hand, is purely image-based, and thus less complex, fully automatic, and equipped with a face tracking and transfer step that are robust to changes in head pose. Moreover, our image retrieval step works on source and target sequences with notably different performances. In this respect, our method is closely related to the work of Efros *et al*. [10], Kemelmacher-Shlizerman *et al*. [14] and Li *et al*. [16]. As opposed to these works, we do not use a dedicated source database, but only a short sequence of the user performing arbitrary expressions and head motion. Contrary to [14], we further combine appearance and motion similarities in our matching metric to enforce temporally coherent image look-up. Finally, we produce a proper composite of the user's face in the target sequence, while previous works [14] and [16] only produce an, often stop-motion-like, assembly of source frames. Berthouzoz *et al*. [3] use hierarchical clustering to find frames of similar expression and head pose to produce smooth transitions between video segments, but the obtained clusters lack temporal continuity. Expression mapping [17] is another related technique, which transfers a target expression to a neutral source face. However, this technique does not preserve the target head motion and illumination, and has problems inside the mouth region, where teeth are not visible. Furthermore, our image retrieval step transfers subtle details of the user's facial expressions, which can differ between individual users.

3. Overview of our Face Reenactment System

Our system takes as input two videos showing facial performances of two different persons: a *source sequence* $\mathcal{S}$ of the user, and a *target sequence* $\mathcal{T}$ of an actor. The goal is to replace the actor's inner face region with that of the user, while preserving the target performance, scene appearance and lighting as faithfully as possible. The result is the *reenactment sequence* $\mathcal{R}$. The source and target video are not assumed to depict the same performance: We can

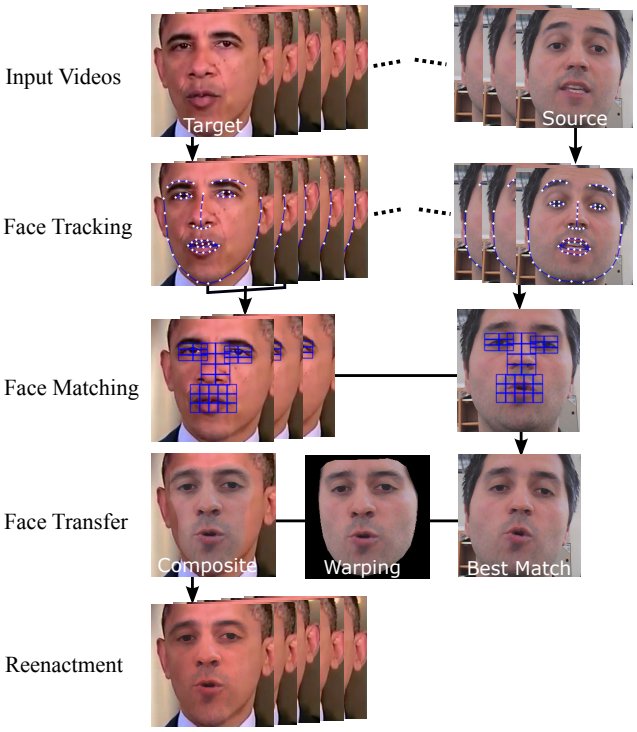

Figure 1. Overview of the proposed system.

produce reenactments for different target videos from only a single source video, which is assumed to show the user going through a short series of random facial expressions while facing the camera. The target sequence can be general footage depicting a variety of expressions and head poses.

Our approach consists of three subsequent steps (Fig. 1):

1. *Face Tracking* (Sec. 4): A non-rigid face tracking algorithm tracks the user and actor throughout the videos and provides facial landmark points. These landmarks are stabilized to create a sequence of annotated frames.

2. *Face Matching* (Sec. 5): The appearance of the main facial regions is encoded as a histogram of local binary patterns, and target and source frames are matched by a nearest neighbor search. This is rendered more stable by dividing the target sequence into chunks of similar appearance and taking into account face motion.

3. *Face Transfer* (Sec. 6): The target head pose is transferred to the selected source frames by warping the facial landmarks. A smooth transition is created by synthesizing in-between frames, and blending the source face into the target sequence using seamless cloning.

4. Non-Rigid Face Tracking

To track user and actor in the source and target sequence, respectively, we utilize a non-rigid 2D face tracking algorithm proposed by Saragih *et al*. [20], which tracks $n = 66$ consistent landmark locations on the human face (eyes, nose, mouth, and face outline, see Fig. 2 (a)). The approach is an instance of the constrained local model (CLM) [8], using the subspace constrained mean-shift algorithm as an optimization strategy. Specifically, it is based on a 3D point distribution model (PDM), which linearly models non-rigid shape variations around 3D reference landmark locations, $\bar{\boldsymbol{X}}_i$, $i = 1, \ldots, n$, and composes them with a global rigid transformation:

$$\boldsymbol{x}_i = sPR\left(\bar{\boldsymbol{X}}_i + \Phi_i \boldsymbol{q}\right) + \boldsymbol{t} \ . \tag{1}$$

Here, $\boldsymbol{x}_i$ is the estimated 2D location of the i-th landmark, and s, R, $\boldsymbol{t}$ and $\boldsymbol{q}$ the PDM parameters, corresponding to the scaling, the 3D rotation, the 2D translation, and the non-rigid deformation parameters. Further, Φ_i denotes the sub-matrix of the basis of variation to the i-th landmark and P is the orthogonal projection matrix. To find the most likely landmark locations, the algorithm uses trained local feature detectors in an optimization framework that enforces a global prior over the combined landmark motion. We remark that we only use the 2D landmark output $(\boldsymbol{x}_1, ..., \boldsymbol{x}_n)$ of the tracker, and not the underlying 3D PDM.

The facial landmarks are prone to noise and inaccuracies, especially for expressions on which the face tracker was not trained. This can render the face matching (see Sec. 5) and face transfer (see Sec. 6) less stable. To increase tracking accuracy, we therefore employ a correction method similar to that proposed by Garrido *et al*. [12], which refines the landmark locations using optical flow between automatically selected key frames, i.e., frames for which the localization of the facial features detected by the face tracker is reliable, such as a neutral expression. To improve the smoothness of the landmark trajectories, we do not use the estimated optical flow value at the exact landmark location $\boldsymbol{x}_i$, like Garrido *et al*., but assign a weighted average of the flow in a circular neighborhood around $\boldsymbol{x}_i$. This neighborhood of size $r \cdot p$ is built by distributing p points evenly on circles with radial distances of $1, 2, \ldots, r$ from $\boldsymbol{x}_i$. In our experiments we choose $r = 2$ and $p = 8$, and weigh the flow values by a normalized Gaussian centered at $\boldsymbol{x}_i$.

5. Face Matching

A central part of our reenactment system is matching the source and target faces under differences in head pose. Here, we find a trade-off between exact expression matching, and temporal stability and coherence. The tracking step of the previous section provides us with facial landmarks which represent the face shape. Instead of comparing shapes directly, we match faces based on appearance and landmark motion, depicting the facial expression and its rate of change, respectively. Another contribution of the matching step is a temporal clustering approach that renders the matching process more stable.

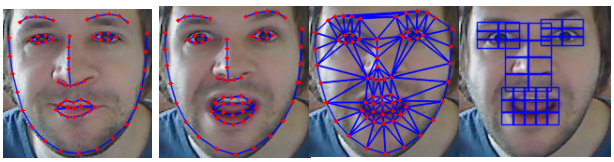

(a) (b)

Figure 2. (a) Annotated reference frame. (b) Expressive face aligned to the reference. Left to right: estimated landmarks, triangulation, and detected regions of interest. The mouth, eyes and nose regions are split into 3×5, 3×2 and 4×2 tiles, respectively.

5.1. Image Alignment and Feature Extraction

Before extracting meaningful facial features, the source and target frames are first aligned to a common reference frame. For this purpose, we choose the first frame in the source sequence, which is assumed to depict the user at rest. Unlike methods that align source and target using a morphable 3D model [14], we compute a 2D affine transformation for each frame that optimally maps the set of detected landmarks onto the reference shape. Since this transformation is global, it does not change the expression in the aligned frames. This alignment is only necessary for the temporal clustering and frame selection of Sec. 5.2, but is not applied for the subsequent steps of our system.

To extract facial features in the aligned frames, we consider four regions of interest of fixed size, which are computed as the bounding boxes of the landmark locations corresponding to the mouth, eyes and nose in the reference frame. After padding these regions by 10 pixels, we split them into several tiles, as shown in Fig. 2. As feature descriptor for a region of interest, we choose histograms of Local Binary Patterns (LBPs) [18], which have been found suitable for tasks such as texture classification and face recognition [1, 14, 22, 15]. An LBP encodes the relative brightness around a given pixel by assigning a binary value to each neighboring pixel, depending on whether its intensity is brighter or darker. The result is an integer value for the center pixel between 0 and 2^l, where l is the number of pixels in a circular neighborhood. We use a uniform code [14], which assigns an own label to every combination for which the number of transitions between 0 and 1 is at most two, and a single label for all other combinations. For a neighborhood size of $l = 8$, this results in an LBP histogram h of 59 bins for each tile. Empirically, we found that a uniform code lacks in discriminative power to match expressions from a wider set other than the distinctive neutral, sadness, happiness, anger, etc. To include information at a finer scale of detail, we additionally compute a normal LBP histogram for a neighborhood size of $l = 4$, thereby extending h to 75 bins. By concatenating the histograms for all m tiles that make up a region of interest, an LBP feature descriptor $H = (h_1, \ldots, h_m)$ for that region is created.

5.2. Temporal Clustering and Frame Selection

Matching source and target frames directly may lead to abrupt frame-to-frame expression changes in the reenactment. The reasons for this are: 1) We experienced a sensitivity of LBP feature descriptors w.r.t. the detected regions of interest, which can result in slightly different source selections for similar target expressions (comparable effects were reported by Li *et al.* [16]). 2) The source sequence is sparse and may not contain an exact match for each target expression. 3) There is no temporal consistency in the image selection. To overcome these shortcomings, we stabilize the matching process by a temporal clustering approach, which finds the source frame that is most similar to a small section of target frames. Additionally, we enforce temporal continuity by extending the appearance metric with a motion similarity term, which takes into account the change in expression.

Temporal Clustering. To stabilize the selection of source frames, we divide the target sequence into consecutive sections of similar expression and appearance, and look for the source frame that best matches a whole target section. To measure the similarity between two consecutive target frames $f_\mathcal{T}^t, f_\mathcal{T}^{t+1} \in \mathcal{T}$, we compute the *appearance distance*

$$d_{\text{app}}(f_\mathcal{T}^t, f_\mathcal{T}^{t+1}) = \sum_{j=1}^{4} w_j \, d_{\chi^2}\left(H_j(f_\mathcal{T}^t), H_j(f_\mathcal{T}^{t+1})\right) \quad , \quad (2)$$

where $H_j(f)$ is the LBP feature descriptor for the j-th of the four regions of interest in f, w_j an accompanying weight, and d_{χ^2} the normalized chi-squared distance between two histograms. The weights for mouth, eyes and nose regions were experimentally set to 0.6, 0.15 and 0.1, respectively.

We propose an agglomerative clustering approach that preserves temporal continuity and proceeds hierarchically. Assuming that each frame is initially a separate cluster, each subsequent iteration joins the two consecutive clusters that are closest according to the metric in Eq. (2). As a linkage criterion, the appearance distance between two consecutive clusters $\mathcal{C}_1$ and $\mathcal{C}_2$ is defined as the average of the pairwise distances d_{app} between all frames in $\mathcal{C}_1$ and all frames in $\mathcal{C}_2$. The two clusters are merged if 1) they only contain a single frame or 2) the variance of d_{app} within the merged cluster is smaller than the maximum of the variances within the separate clusters. The last criterion keeps the frames within a cluster as similar as possible, and once it is not met, the algorithm terminates. The result is a sequence of target sections $\mathcal{C}^k$, with k an index running in temporal direction over the number of clusters. We observed that the length of a cluster $\mathcal{C}$ varies inversely proportionally to the change in expression and the timing of speech within $\mathcal{C}$ (see the supplemental material for an analysis of the number of detected clusters and their lengths).

Frame Selection. To select a source frame $f_{\mathcal{S}}^k \in \mathcal{S}$ that matches a target section $\mathcal{C}^k$, we compute an aggregated similarity metric over all target frames in a cluster:

$$d(\mathcal{C}, f_{\mathcal{S}}) = \sum_{f_{\mathcal{T}} \in \mathcal{C}} d_{\text{app}}(f_{\mathcal{T}}, f_{\mathcal{S}}) + \tau \; d_{\text{mot}}(\boldsymbol{v}_{\mathcal{C}}, \boldsymbol{v}_{\mathcal{S}}) \;\; . \quad (3)$$

Here, $d_{\text{app}}(f_1, f_2)$ is the appearance distance defined in Eq. (2) and $d_{\text{mot}}(\boldsymbol{v}_1, \boldsymbol{v}_2)$ a *motion distance* that measures the similarity between two vector fields. The vector field $\boldsymbol{v}_{\mathcal{C}}$ describes the motion of the n facial landmarks between two consecutive clusters. The motion of the i-th landmark $\boldsymbol{v}_{\mathcal{C}i}$ is computed as the difference of its average positions in the current cluster $\mathcal{C}^k$ and the previous cluster $\mathcal{C}^{k-1}$. The vector field $\boldsymbol{v}_{\mathcal{S}}$ describes the motion of the n facial landmarks between two consecutively selected source frames, i.e. for the i-th landmark, $\boldsymbol{v}_{\mathcal{S}i}$ is the difference of its position in $f_{\mathcal{S}}^k$ and $f_{\mathcal{S}}^{k-1}$. Note that $\boldsymbol{v}_{\mathcal{C}}$ and $\boldsymbol{v}_{\mathcal{S}}$ are computed for normalized landmark locations in the aligned source and target frames. The motion distance d_{mot} is defined as

$$d_{\text{mot}}(\boldsymbol{v}_{\mathcal{C}}, \boldsymbol{v}_{\mathcal{S}}) = 1 - \frac{1}{3} \sum_{j=1}^{3} \exp\big(- d_j(\boldsymbol{v}_{\mathcal{C}}, \boldsymbol{v}_{\mathcal{S}})\big) \;\; , \quad (4)$$

where $d_1 = \frac{1}{n} \sum_i \|\boldsymbol{v}_{\mathcal{C}i} - \boldsymbol{v}_{\mathcal{S}i}\|$ measures the Euclidean distance, $d_2 = \frac{1}{n} \sum_i (1 - \boldsymbol{v}_{\mathcal{C}i} \cdot \boldsymbol{v}_{\mathcal{S}i} / \|\boldsymbol{v}_{\mathcal{C}i}\| \|\boldsymbol{v}_{\mathcal{S}i}\|)$ the angular distance, and $d_3 = \frac{1}{n} \sum_i \big| \|\boldsymbol{v}_{\mathcal{C}i}\| - \|\boldsymbol{v}_{\mathcal{S}i}\| \big|$ the difference in magnitude between the motion fields $\boldsymbol{v}_{\mathcal{C}}$ and $\boldsymbol{v}_{\mathcal{S}}$. The motion distance d_{mot} therefore measures how similar the change in expression in the selected source frames is compared to the change in expression between target clusters. It is important to understand that consecutively selected frames $f_{\mathcal{S}}^{k-1}$ and $f_{\mathcal{S}}^k$ do not have to be consecutive in the original source sequence $\mathcal{S}$. Our matching metric is thus suitable for source and target sequences that have an entirely different timing and speed. Both the aggregated appearance distance and motion distance in Eq. (3) are normalized to $[0, 1]$ and the weighting factor τ was set to 0.8 for all experiments.

Given $f_{\mathcal{S}}^{k-1}$, the source frame with the minimal total distance $d(\mathcal{C}^k, f_{\mathcal{S}})$ over all $f_{\mathcal{S}} \in \mathcal{S}$, is chosen as the best match $f_{\mathcal{S}}^k$ and assigned to the central timestamp of $\mathcal{C}^k$. If $\mathcal{C}^k$ consists of a single frame, $f_{\mathcal{S}}^k$ is assigned to this timestamp.

6. Face Transfer

After selecting the best representative source frames, we transfer the face of the user to the corresponding target frames and create the final composite. First, we employ a 2D warping approach which combines global and local transformations to produce a natural shape deformation of the user's face that matches the actor in the target sequence. The estimated shape is then utilized to transfer the user's appearance and synthesize a compelling transition.

6.1. Shape and Appearance Transfer

While only methods relying on complex 3D face models can handle large differences in head pose between source and target [9], we present a simple, yet effective, image-based strategy that succeeds in such cases. Inspired by work on template fitting [5, 26], we formulate face transfer as a deformable 2D shape registration that finds a user shape and pose that best correspond to the shape and pose of the actor, while preserving the user's identity as much as possible.

Shape Transfer. For each target frame $f_{\mathcal{T}}^t \in \mathcal{T}$, we want to estimate the n 2D landmark locations $(\boldsymbol{x}_{\mathcal{R}1}^t, ..., \boldsymbol{x}_{\mathcal{R}n}^t)$ of the user's face in the reenactment sequence $\mathcal{R}$. To achieve this, we propose a warping energy composed of two terms: a non-rigid term and an affine term. The non-rigid term penalizes deviations from the target shape:

$$E_{\text{nr}} = \sum_{i=1}^{n} \Big\| \boldsymbol{x}_{\mathcal{R}i}^t - \big(\alpha_1 \, \boldsymbol{x}_{\mathcal{T}i}^{t-1} + \alpha_2 \, \boldsymbol{x}_{\mathcal{T}i}^{t} + \alpha_3 \, \boldsymbol{x}_{\mathcal{T}i}^{t+1}\big) \Big\|^2 \;\; , \quad (5)$$

where $\boldsymbol{x}_{\mathcal{T}i}^t$ denotes the i-th landmark in the target frame at time t and α_j, $\sum_j \alpha_j = 1$, are normalized weights (0.1, 0.8 and 0.1 in our experiments). The affine term penalizes deviations from the selected source shape:

$$E_{\text{r}} = \sum_{i=1}^{n} \Big\| \boldsymbol{x}_{\mathcal{R}i}^t - \big(\beta_1 \, M^{k-1} \boldsymbol{x}_{\mathcal{S}i}^{k-1} + \beta_2 \, M^{k} \boldsymbol{x}_{\mathcal{S}i}^{k}\big) \Big\|^2 \;\; , \quad (6)$$

where $\boldsymbol{x}_{\mathcal{S}i}^{k-1}$ (resp. $\boldsymbol{x}_{\mathcal{S}i}^{k}$) is the i-th landmark in the selected source frame immediately preceding (resp. following) the current timestamp t, and M a global affine transformation matrix which optimally aligns the corresponding source and target shapes. As the selected source frames are only assigned to the central timestamp of a temporal cluster, no selected source shape may correspond to the current target frame $f_{\mathcal{T}}^t$, so this term effectively interpolates between the closest selected source shapes, thereby preserving the user's identity. The weights β_j, $\sum_j \beta_j = 1$, depend linearly on the relative distance from t to the central timestamps of $\mathcal{C}^{k-1}$ and $\mathcal{C}^k$, being 0 or 1 if t coincides with one of the cluster centers. Combining the two terms together with their corresponding weights w_{nr} and w_{r}, yields the total energy

$$E_{\text{tot}}(\boldsymbol{x}_{\mathcal{R}i}^t) = w_{\text{nr}} \, E_{\text{nr}} + w_{\text{r}} \, E_{\text{r}} \;\; , \quad (7)$$

where $w_{\text{nr}} + w_{\text{r}} = 1$. A closed-form solution to Eq. (7) for the optimal landmark locations $(\boldsymbol{x}_{\mathcal{R}1}^t, ..., \boldsymbol{x}_{\mathcal{R}n}^t)$ exists.

Appearance Transfer. Once we have the optimal shape of the face in the reenactment sequence, we transfer the appearance of the selected source frames by inverse-warping the corresponding source texture [21] using a triangulation of the landmark points (see Fig. 2 (b)). For the in-between

Figure 3. Comparison of warping approaches. Left: Selected user frame. Right: Target pose. Middle left to right: non-rigid warping (Eq. (5)), affine warping (Eq. (6)), and our approach (Eq. (7)).

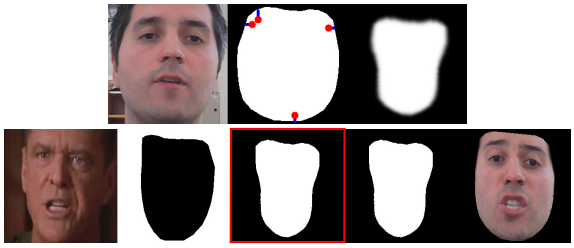

Figure 4. Seam generation. Top: User at rest, source mask with landmarks closest to the boundary in red, and eroded mask. Bottom left: Target frame and mask. Bottom Right: Transferred source frame and mask. Bottom middle: Final blending seam.

frames, we create a smooth transition in appearance by interpolating the texture from the closest selected source frames using the same triangulation of the landmarks.

Note that a shape and appearance transfer as described here are generally not possible with conventional warping approaches, such as global non-rigid warping and global affine warping, as shown in Fig. 3. The former creates unrealistic distortions in texture since it fits the source shape exactly to the target shape, while the latter may fail under strong perspective views and create odd deformations whenever the source and target shape do not agree.

6.2. Compositing

We produce a convincing composite, where the main facial source features, represented by the eyes, nose, mouth, and chin are seamlessly implanted on the target actor. The lighting of the target sequence, and the skin appearance and hair of the target actor, should be preserved. For this purpose we use Poisson seamless cloning [19]. We create a tight binary mask for the source sequence containing the main facial features of the user at rest, such as eyes, mouth, nose and eyebrows. We then perform an erosion with a Gaussian structuring element that is constrained by the landmark locations in the facial features. Thresholding this mask gives us a seam for blending (see Fig. 4, top).

To obtain a seam for each frame in the reenactment, the precomputed source mask is transferred by inverse-warping (see Sec. 6.1). We prevent the seam from running outside the target face by intersecting it with a mask containing the main facial features of the target actor (see Fig. 4, bottom). For increased insensitivity to the source illumination, we transform the source and target frames into the perception-based color space of [7] before performing Poisson blending [19]. The blended image is converted back to RGB space, resulting in the final composite (see Fig. 1). To avoid artifacts across the seam, we blend the boundary pixels using a Gaussian with a standard deviation of 9 pixels.

7. Results

We evaluate our method on two types of data: We use videos that were prerecorded in a studio with an SLR camera to demonstrate the reenactment quality on existing high-quality footage. We also reenact faces in videos taken from the Internet using a random performance of a user captured with a webcam. This demonstrates our system's ease of use and its applicability to online content. Our system was implemented in C++ and tested on a 3.4 GHz processor.

Existing Video. We recorded two male and two female users performing random facial gestures and speech under similar ambient lighting to simulate existing high-quality HD footage. As source sequences, we selected a snippet of about 10 s from the first two recordings and used the second recordings as target. Fig. 5 shows the two reenactment results of 22 and 12 s. Note that our system is able to reproduce the target performance in a convincing way, even when head motion, expression, timing, and speech of user and actor differ substantially. Computation time for the face tracking step was about 4 s per frame, while the combined face matching and face transfer took 4.5 min in total for both results. To appreciate the temporal quality of these and additional results, we refer to the supplementary video.

Low-Quality Internet Video. Fig. 6 shows results for two target videos downloaded from the Internet. The user recorded himself with a standard webcam (20 fps, 640×480) for 10 s, and the reenactments were produced for subsequences of 18 and 8 s. Both target videos exhibit different speech, head pose, lighting and resolution than the recorded source sequence. Our system nevertheless produces plausible animations, even in the presence of quite some head motion, such as in the Obama sequence. Face matching and face transfer took between 4 and 7 min.

Validation. A user study in the supplementary material shows with statistical significance that our temporal clustering of Sec. 5.2 and combined appearance and motion distance of Eq. (3) outperform a frame-by-frame matching with the appearance metric of Eq. (2). Reenactment results for 5 existing and 2 web videos were rated by 32 participants w.r.t. the original target performance in terms of mim-

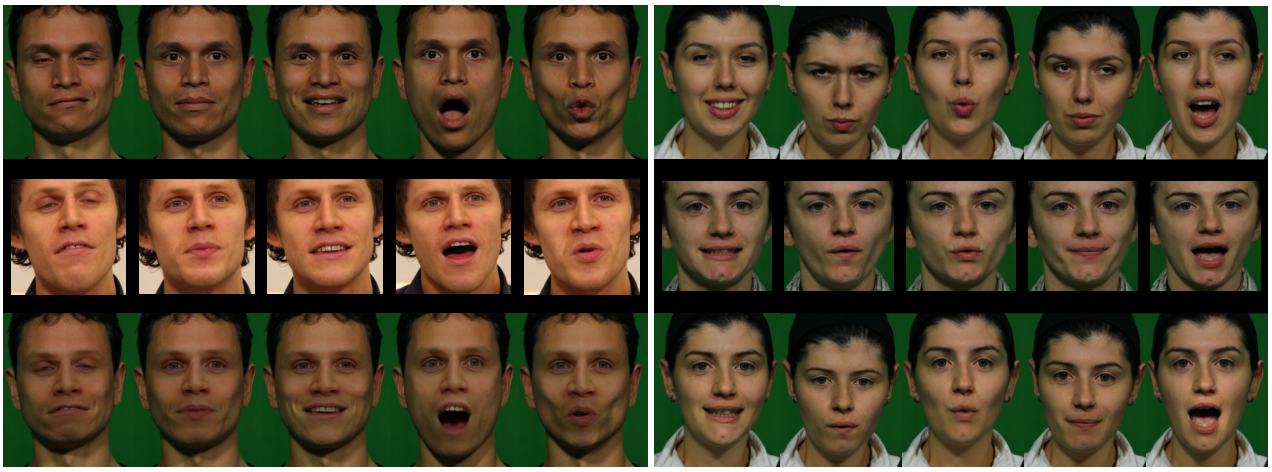

Figure 5. Existing HD video (22 s on the left, 12 s on the right). Top: Example frames from the target sequence. Middle: Corresponding selected source frames. Bottom: Final composite. Weights in Eq. (7): $w_{\text{nr}} = 0.65$, $w_{\text{r}} = 0.35$ (left) and $w_{\text{nr}} = 0.55$, $w_{\text{r}} = 0.45$ (right).

Figure 6. Low-quality Internet video (18 s from Obama's speech on the left (http://youtu.be/qxtydXN3f1U), 8 s excerpt from "A Few Good Men" on the right (http://youtu.be/5j2F4VcBmeo)). Top: Example frames from the target sequence. Middle: Corresponding selected source frames. Bottom: Final composite. Weights in Eq. (7): $w_{\text{nr}} = 0.65$, $w_{\text{r}} = 0.35$ (left) and $w_{\text{nr}} = 0.45$, $w_{\text{r}} = 0.55$ (right).

icking fidelity, temporal consistency and visual artifacts on a scale from 1 (not good) to 5 (good). The average scores over all results were 3.25 for our full system, 2.92 without temporal clustering and 1.48 without motion distance.

The supplementary material presents an analysis of the source video length, and demonstrates that increasing the amount of source frames improves the quality of the reenactment, both in realism and temporal smoothness. The supplementary material also shows that reenactment and target are almost indistinguishable when source and target are the same sequence. For two such *self-reenactments* of 10 s and 22 s, our system produced 1 and 36 mismatches on 59 and 214 computed clusters, respectively (a mismatch is a selected frame not contained in the cluster). Mismatches were mostly visually very similar to the corresponding cluster centers, such that the final reenactment is close to a perfect frame-by-frame synthesis. Also for the case where source and target depict the same person under similar conditions, the reenactment resembles the target closely.

Finally, we compared our system to the 3D approach of Dale *et al*. [9] on data provided by the authors, depicting two different subjects reciting the same poem. Our automatic reenactment system produces a convincing result that is visually very close in quality to their semi-automatic result. Since the system of Dale *et al*. is designed to transfer the source face together with the complete source performance, while our approach preserves the target performance, both results might differ slightly in a frame-by-frame comparison (see the supplementary video).

Discussion. Despite differences in speech, timing and lighting, our system creates credible animations, provided that the lighting remains constant or changes globally. Local variations can lead to wrong color propagation across the seam and can produce flicker and less realistic reenactments. Ghosting artifacts may also appear in the mouth

region stemming from blending and temporal inconsistencies. In the future, we aim to drive the mouth separately, and make the compositing step more robust to lighting changes.

Although our aim is to closely reproduce the facial expressions in the target sequence, our reenactment results can differ from the original performance due to the source sequence not containing a matching expression, or the limited precision of our matching metric. Even under perfect matching conditions, our system will preserve person-specific nuances and subtle specialties of the source expressions, which not only differ in detail from the target expressions, but also between individual users of the system.

8. Conclusion

We proposed an image-based reenactment system that replaces the inner face of an actor in a video, while preserving the original facial performance. Our method requires no user interaction, nor a complex 3D face model. It is based on expression matching and uses temporal clustering for matching stability and a combined appearance and motion metric for matching coherence. A simple, yet effective, image-warping technique allowed us to deal with moderate head motion. Experiments showed convincing reenactment results for existing footage, obtained by using only a short input video of a user making arbitrary facial expressions.

Acknowledgments

This research was supported by the ERC Starting Grant CapReal (grant agreement 335545) and by Technicolor.

References

[1] T. Ahonen, A. Hadid, and M. Pietikainen. Face description with local binary patterns: Application to face recognition. *IEEE TPAMI*, 28(12):2037–2041, 2006.

[2] O. Alexander, M. Rogers, W. Lambeth, M. Chiang, and P. Debevec. The Digital Emily Project: photoreal facial modeling and animation. In *ACM SIGGRAPH Courses*, pages 12:1–12:15, 2009.

[3] F. Berthouzoz, W. Li, and M. Agrawala. Tools for placing cuts and transitions in interview video. *ToG (Proc. SIGGRAPH)*, 31(4):67:1–67:8, 2012.

[4] D. Bitouk, N. Kumar, S. Dhillon, P. Belhumeur, and S. K. Nayar. Face swapping: Automatically replacing faces in photographs. *ToG (Proc. SIGGRAPH)*, 27(3):39:1–39:8, 2008.

[5] V. Blanz, K. Scherbaum, T. Vetter, and H.-P. Seidel. Exchanging faces in images. *Comp. Graph. Forum*, 23(3):669–676, 2004.

[6] C. Bregler, M. Covell, and M. Slaney. Video rewrite: driving visual speech with audio. *ToG (Proc. SIGGRAPH)*, pages 353–360, 1997.

[7] H. Y. Chong, S. J. Gortler, and T. Zickler. A perception-based color space for illumination-invariant image processing. *ToG (Proc. SIGGRAPH)*, 27(3):61:1–61:7.

[8] D. Cristinacce and T. F. Cootes. Feature detection and tracking with constrained local models. In *Proc. BMVC*, pages 929–938, 2006.

[9] K. Dale, K. Sunkavalli, M. K. Johnson, D. Vlasic, W. Matusik, and H. Pfister. Video face replacement. *ToG (Proc. SIGGRAPH Asia)*, 30(6):130:1–130:10, 2011.

[10] A. A. Efros, A. C. Berg, G. Mori, and J. Malik. Recognizing action at a distance. In *Proc. ICCV*, pages 726–733, 2003.

[11] P. Eisert and B. Girod. Analyzing facial expressions for virtual conferencing. *Computer Graphics and Applications*, 18(5):70–78, 1998.

[12] P. Garrido, L. Valgaerts, C. Wu, and C. Theobalt. Reconstructing detailed dynamic face geometry from monocular video. *ToG (Proc. SIGGRAPH Asia)*, 32(6):158:1–158:10, 2013.

[13] A. Jones, J. Chiang, A. Ghosh, M. Lang, M. Hullin, J. Busch, and P. Debevec. Real-time geometry and reflectance capture for digital face replacement. Technical Report 4s, University of Southern California, 2008.

[14] I. Kemelmacher-Shlizerman, A. Sankar, E. Shechtman, and S. M. Seitz. Being John Malkovich. In *Proc. ECCV*, volume 6311 of *LNCS*, pages 341–353. 2010.

[15] I. Kemelmacher-Shlizerman, E. Shechtman, R. Garg, and S. M. Seitz. Exploring photobios. *ToG (Proc. SIGGRAPH)*, 30(4):61:1–61:10, 2011.

[16] K. Li, F. Xu, J. Wang, Q. Dai, and Y. Liu. A data-driven approach for facial expression synthesis in video. In *Proc. CVPR*, pages 57–64, 2012.

[17] Z. Liu, Y. Shan, and Z. Zhang. Expressive expression mapping with ratio images. *ToG (Proc. SIGGRAPH)*, pages 271–276, 2001.

[18] T. Ojala, M. Pietikäinen, and T. Mäenpää. Multiresolution gray-scale and rotation invariant texture classification with local binary patterns. *IEEE TPAMI*, 24(7):971–987, 2002.

[19] P. Pérez, M. Gangnet, and A. Blake. Poisson image editing. *ToG (Proc. SIGGRAPH)*, 22(3):313–318, 2003.

[20] J. M. Saragih, S. Lucey, and J. F. Cohn. Face alignment through subspace constrained mean-shifts. In *Proc. ICCV*, pages 1034–1041, 2009.

[21] J. M. Saragih, S. Lucey, and J. F. Cohn. Real-time avatar animation from a single image. In *Automatic Face and Gesture Recognition Workshops*, pages 213–220, 2011.

[22] X. Tan and B. Triggs. Enhanced local texture feature sets for face recognition under difficult lighting conditions. *IEEE TIP*, 19(6):1635–1650, 2010.

[23] B.-J. Theobald, I. Matthews, M. Mangini, J. R. Spies, T. R. Brick, J. F. Cohn, and S. M. Boker. Mapping and manipulating facial expression. *Language and Speech*, 52(2–3):369–386, 2009.

[24] D. Vlasic, M. Brand, H. Pfister, and J. Popović. Face transfer with multilinear models. *ToG (Proc. SIGGRAPH)*, 24(3):426–433, 2005.

[25] T. Weise, S. Bouaziz, H. Li, and M. Pauly. Realtime performance-based facial animation. *ToG (Proc. SIGGRAPH)*, 30(4):77:1–77:10, 2011.

[26] T. Weise, H. Li, L. J. V. Gool, and M. Pauly. Face/Off: live facial puppetry. In *Proc. SIGGRAPH/Eurographics Symposium on Computer Animation*, pages 7–16, 2009.